AIAA JOURNAL
Vol. 45, No. 9, September 2007

Technical Notes

TECHNICAL NOTES are short manuscripts describing new developments or important results of a preliminary nature. These Notes should not exceed 2500 words (where a figure or table counts as 200 words). Following informal review by the Editors, they may be published within a few months of the date of receipt. Style requirements are the same as for regular contributions (see inside back cover).

Multidomain Spectral Collocation Method for Stability Analysis of Detonations

Anatoli Tumin*
University of Arizona, Tucson, Arizona, 85721

DOI: 10.2514/1.29722

I. Introduction

THE hydrodynamic stability of detonations is a relatively new area of study in fluid mechanics. It was founded by J. J. Erpenbeck in 1962 [1]. Erpenbeck formulated the stability problem as an initial-value problem for the linearized reactive Euler equations with conservation conditions at the shock front. A formal solution of the initial-value problem was found with the help of the Laplace transform with respect to time. It was shown that the solution may have poles in the right-hand side of the Laplace variable plane, which means instability of the flow. A dispersion relation for the poles was formulated explicitly in terms of integrals and functions that are to be found as solutions of ordinary differential equations. Instead of directly solving the dispersion relation numerically, Erpenbeck used the *principle of the argument* to establish the existence of the poles in the case of idealized one-reaction detonations [2]. (More references relevant to the early stages of the stability theory of detonations are given by Fickett and Davis [3].)

Systematic studies of the discrete spectrum in a variety of detonation stability problems using the normal-mode approach were started by Lee and Stewart [4]. The normal-mode analysis leads to an inhomogeneous system of linear ordinary differential equations in the shock wave coordinates. Lee and Stewart integrated the system, starting with the postshock values $x = 0_+$ for the velocity, pressure, specific volume, and reaction progress variable perturbations. At the end of the reaction zone $x \to +\infty$, the solution boundedness constraint was formulated as an algebraic relation for the perturbations. This constraint served as the dispersion relation, solved with the help of a shooting algorithm. Later on, the normal-mode approach was used in a number of problems by other researchers [5–8]. It is shown in [9] that the discrete spectrum stemming from the solution of the initial-value problem is equivalent to the spectrum of the normal-mode approach, and that the boundedness constraint at $x \to +\infty$ can be easily derived from Erpenbeck's solution [1].

Because the shooting procedure is sensitive to the initial guess, application of Lee and Stewart's [4] method requires a "carpet search." In many other hydrodynamic stability problems, eigenvalue analysis is often accompanied by the spectral collocation method. The method provides an eigenvalue map without an initial guess. To our knowledge, the spectral collocation method has not found wide application in studies of detonation stability. Buckmaster and Neves [10] used a spectral collocation method with Chebyshev polynomials for a case of infinite activation energy. The problem formulation led to equations with constant steady-state variables within the induction zone. Namah et al. [11] applied a spectral collocation method to the analysis of one-dimensional detonations at finite activation energy. They decided that the shock-fixed frame was not suitable for an adopted numerical scheme, and they formulated the governing equations in the inertial frame. The numerical results of [11] were obtained with only 128 collocation points, and the authors noticed that their collocation scheme distributes points rather thinly in regions where the reaction progress variable changes just a little.

The objective of the present work is to use the multidomain spectral collocation method with Chebyshev polynomials [12] and to demonstrate the efficiency of the method for stability analysis of detonations.

II. Problem Formulation

For simplicity of the method description, consider one-dimensional perturbations in a one-dimensional flow of an ideal gas that participates in a first-order, irreversible reaction without mole and specific heat change. It means that the gas constant R_g and the specific heat ratio γ are the same in the freestream and in the reaction zone.

One can find the dimensionless steady-state distributions of pressure p^*, velocity u^*, and specific volume v^* in [4]:

$$p^* = a + (1-a)\sqrt{1 - b\beta\lambda^*}, \qquad u^* = \frac{(1-p^*)}{\gamma M_s} + M_s \qquad v^* = \frac{u^*}{M_s} \tag{1}$$

where λ is the reaction progress variable ($0 \le \lambda \le 1$), the superscript $*$ indicates the steady-state solution, and a and b are constants

$$a = \frac{1+\gamma D^2}{2\gamma M_s^2 - (\gamma - 1)}, \qquad b = \frac{2\gamma M_s^2(\gamma-1)}{(1-a)^2(\gamma+1)} \tag{2}$$

We use the same scaling as in [4]. Density ρ_s, pressure p_s, and speed of sound behind the shock c_s are used as the dimensional scales. The half-reaction zone length l_c is chosen as the characteristic length scale. The time scale is $t_c = l_c/c_s$. The steady dimensionless detonation velocity D is scaled with the speed of sound in the quiescent gas, and M_s is the Mach number of the flow behind the shock in the frame moving with the shock wave. The dimensionless heat release $\beta = \tilde{Q}/R_g T_s$ is based on the temperature behind the shock T_s. The dimensionless reaction rate is

$$r^* = k(1-\lambda^*)\exp(-\theta/T^*) \qquad \theta = \tilde{E}/R_g T_s \qquad k = \int_0^{1/2} u^*(1-\lambda^*)^{-1}\exp(\theta/T^*)\,\mathrm{d}\lambda^* \tag{3}$$

The steady-state flow is characterized by the overdrive factor $f = (D/D_{CJ})^2$, where

Received 12 January 2007; revision received 1 May 2007; accepted for publication 7 May 2007.

*Professor, Department of Aerospace and Mechanical Engineering. AIAA Associate Fellow.

$$D_{\mathrm{CJ}} = \sqrt{1 + \frac{(\gamma^2 - 1)Q}{2\gamma}} + \sqrt{\frac{(\gamma^2 - 1)Q}{2\gamma}} \tag{4}$$

is the Chapman–Jouguet detonation velocity and $Q = \tilde{Q}/R_g T_1$ is the dimensionless heat release scaled with the help of the quiescent gas temperature T_1.

Following [1], the governing equations for perturbations are obtained in the wave coordinate $x = x^l - D_s t - \psi(t)$, where D_s is the detonation shock velocity scaled with the speed of sound behind the shock and $\psi(t)$ is the shock displacement. The particle velocity is measured with respect to the steady frame $u = u^l - D_s$. One can derive the linearized equations for perturbations [$\sim \exp(\alpha t)$] in the notation of [4] as follows:

$$\alpha z + \mathbf{A}^* \frac{dz}{dx} + \mathbf{C}^* z = \alpha \boldsymbol{b}^* \psi \tag{5a}$$

$$z(0) = \boldsymbol{h}\alpha\psi \tag{5b}$$

where

$$\mathbf{A}^* = \begin{pmatrix} u^* & -v^* & 0 & 0 \\ 0 & u^* & v^*/\gamma & 0 \\ 0 & \gamma p^* & u^* & 0 \\ 0 & 0 & 0 & u^* \end{pmatrix}, \qquad \boldsymbol{b}^* = \begin{pmatrix} \partial v^*/\partial x \\ \partial u^*/\partial x \\ \partial p^*/\partial x \\ \partial \lambda^*/\partial x \end{pmatrix}$$

$$\mathbf{C}^* = \begin{pmatrix} -\partial u^*/\partial x & \partial v^*/\partial x & 0 & 0 \\ (\partial p^*/\partial x)/\gamma & \partial u^*/\partial x & 0 & 0 \\ -\kappa^*(\partial r^*/\partial v - r^*/v^*) & (\partial p^*/\partial x) & \gamma \partial u/\partial x - \kappa^*(\partial r^*/\partial p) & -\kappa^*(\partial r^*/\partial \lambda) \\ -\partial r^*/\partial v & \partial \lambda^*/\partial x & -\partial r^*/\partial p & -\partial r^*/\partial \lambda \end{pmatrix}$$

and $\kappa^* = (\gamma - 1)\beta/v^*$. The column-vector $\boldsymbol{z}$ is composed of perturbations of specific volume, velocity, pressure, and the reaction progress variable. The column-vector $\boldsymbol{h}$ in Eq. (5b) is defined by four components:

$$h_1 = \frac{4}{(\gamma + 1)D^2 M_s}, \qquad h_2 = \frac{2(D^2 + 1)}{(\gamma + 1)D^2}, \qquad h_3 = -\frac{4\gamma M_s}{(\gamma + 1)} \qquad h_4 = 0 \tag{6}$$

At $x \to \infty$, Lee and Stewart [4] formulated a constraint meaning boundedness of the solution (see a discussion in [9])

$$g(\alpha) = \left[M_\infty \zeta_3 + \frac{(D^2 + 1)}{2D^2} \zeta_2 \right] \left[\frac{\alpha}{C_{44}} + (1 - M_\infty) \right] - \zeta_4 M_\infty \frac{\beta(\gamma^2 - 1)}{4\gamma c_\infty} = 0 \tag{7}$$

$$\zeta_2 = \frac{(\gamma + 1)D^2}{2(D^2 + 1)} z_2, \qquad \zeta_3 = -\frac{(\gamma + 1)}{4\gamma M_s} z_3, \qquad \zeta_4 = z_4$$

where z_j stands for the jth component of vector $\boldsymbol{z}$, M_∞ is the Mach number at $x \to \infty$, and c_∞ is the speed of sound at $x \to \infty$ (scaled with the speed of sound behind the shock).

III. Multidomain Spectral Collocation Method

In what follows, we consider overdriven detonation ($f > 1$). In the Chapman–Jouguet detonation wave ($f = 1$), the matrix $\mathbf{A}^*$ is singular at $x \to \infty$. Therefore, the examples with $f = 1$ should be interpreted as results at f slightly greater than one. (Erpenbeck [1] suggested that the result at $f = 1$ be interpreted as "the lower limit in detonation velocity of the overdriven detonations.")

In the overdriven detonation case, the matrix $\mathbf{A}^*$ is nonsingular. Use of the reaction progress variable $\lambda(x)$ as the independent variable leads to the following form of the differential equations:

$$\frac{\mathrm{d}z}{\mathrm{d}\lambda} + \mathbf{D}z = \alpha(\mathbf{F}\psi - \mathbf{E}z) \tag{8a}$$

$$\mathbf{D} = \frac{u^*}{r^*}(\mathbf{A}^*)^{-1}\mathbf{C}^* \tag{8b}$$

$$\boldsymbol{F} = \frac{u^*}{r^*}(\mathbf{A}^*)^{-1}\boldsymbol{b}^* \tag{8c}$$

$$\mathbf{E} = \frac{u^*}{r^*}(\mathbf{A}^*)^{-1} \tag{8d}$$

The multidomain spectral collocation method [12] was used to solve the eigenvalue problem using two and three domains. Instead of boundary condition (7) at $\lambda \to 1$ ($x \to \infty$), we impose the boundedness condition at $\lambda = \lambda_{\max}$ which is slightly less than one. We shall describe the numerical implementation for the case of three domains: 1) $0 \le \lambda \le \lambda_1$, 2) $\lambda_1 \le \lambda \le \lambda_2$, and 3) $\lambda_2 \le \lambda \le \lambda_{\max}$. Each interval is transformed to the computational domain on the Chebyshev interval $-1 \le \xi \le +1$ using algebraic stretching:

Domain 1:

$$\lambda = a_1 \frac{1 + \xi}{b_1 - \xi} \qquad a_1 = \frac{\lambda_{01}\lambda_1}{\lambda_1 - 2\lambda_{01}} \qquad b_1 = 1 + \frac{2a_1}{\lambda_1} \tag{9}$$

Domain 2:

$$\lambda = \lambda_1 + a_2 \frac{1 + \xi}{b_2 - \xi} \qquad a_2 = \frac{(\lambda_{02} - \lambda_1)(\lambda_2 - \lambda_1)}{(\lambda_2 - \lambda_1) - 2(\lambda_{02} - \lambda_1)} \qquad b_2 = 1 + \frac{2a_2}{\lambda_2 - \lambda_1} \tag{10}$$

Domain 3:

$$\lambda = \lambda_2 + a_3 \frac{1 + \xi}{b_3 - \xi} \qquad a_3 = \frac{(\lambda_{03} - \lambda_2)(\lambda_{\max} - \lambda_2)}{(\lambda_{\max} - \lambda_2) - 2(\lambda_{03} - \lambda_2)} \qquad b_3 = 1 + \frac{2a_3}{\lambda_{\max} - \lambda_2} \tag{11}$$

The parameters λ_{01}, λ_{02}, and λ_{03} correspond to $\xi = 0$ for each domain. They are used to control distribution of the collocation points over the domains. The collocation points are defined for the mth domain ($m = 1, 2, 3$) as follows:

$$\xi_j^m = -\cos\frac{\pi j}{N_m}; \qquad (j = 0, \ldots, N_m) \tag{12}$$

(Note the introduced minus sign, which was added so the first node would be at $\xi = -1$.)

At the interfaces of the domains, continuity of the solution is required:

$$z^1|_{\lambda=\lambda_1} = z^2|_{\lambda=\lambda_1}, \qquad \left.\frac{dz^1}{d\lambda}\right|_{\lambda=\lambda_1} = \left.\frac{dz^2}{\lambda d}\right|_{\lambda=\lambda_1} \tag{13}$$

$$z^2|_{\lambda=\lambda_2} = z^3|_{\lambda=\lambda_2}, \qquad \left.\frac{dz^2}{d\lambda}\right|_{\lambda=\lambda_2} = \left.\frac{dz^3}{d\lambda}\right|_{\lambda=\lambda_2} \tag{14}$$

The discretized solution vector $\boldsymbol{Z}$ is composed of $4N_1 + 4N_2 + 4N_3 + 13$ components as follows:

$$\boldsymbol{Z} = (z^1_{10}, \ldots, z^1_{1N_1}, \ldots, z^1_{40}, \ldots, z^1_{4N_1}, z^2_{10}, \ldots, z^2_{1N_2}, \ldots, z^2_{40}, \ldots, z^2_{4N_2}, z^3_{10}, \ldots, z^3_{1N_3}, \ldots, z^3_{40}, \ldots, z^3_{4N_3}, \psi)^T \tag{15}$$

where z_{ij} is the ith component of the vector z at the jth grid point. The derivative $d/d\lambda = (d\xi/d\lambda)d/d\xi$ in Eqs. (8), (13), and (14) is evaluated with the help of the derivative matrix (see, for example, [13]) and the vector values within each domain.

Differential Eq. (8) is satisfied in the interior points of three domains and leads to $4N_1 + 4N_2 + 4N_3 - 12$ equations. In addition, we satisfy Eq. (8) at the endpoint $\lambda = \lambda_{\max}$. Therefore, the discretized differential equation provides $4N_1 + 4N_2 + 4N_3 - 8$ algebraic equations for components of the vector $\boldsymbol{Z}$. Boundary condition (5b) gives four equations. Interface conditions (13) and (14) provide 16 equations. Together with boundary condition (7), we have $4N_1 + 4N_2 + 4N_3 + 13$ algebraic equations written in the form of the generalized eigenvalue problem

$$\mathbf{Q}\,\boldsymbol{Z} = \alpha \mathbf{S}\boldsymbol{Z} \tag{16}$$

where $\mathbf{Q}$ and $\mathbf{S}$ are square matrices of order $4N_1 + 4N_2 + 4N_3 + 13$.

The fourth equation in boundary condition (5b) [see Eq. (6)] and interface conditions (13) and (14) do not include the eigenvalue α. It means that matrix $\mathbf{S}$ is singular. The singularity can be removed by row and column operations and by reducing the order of the system, as was done, for example, in [12]. We have found that the method suggested in [14] is more efficient. We replace the zero rows in the matrix $\mathbf{S}$ by the rows of the matrix $\mathbf{Q}$ multiplied by a small number (usually, we used 10^{-8}). This modification introduces a new eigenvalue ($\alpha = 10^8$ in our case) that is outside the physically interesting domain, whereas the eigenvalues of interest lead to the right-hand side of the equations having the small factor close to zero. Finally, the generalized eigenvalue problem, Eq. (16), can be solved using a standard routine (we used the DG6CCG routine from the International Mathematical and Statistical Library Fortran library).

To explore the effect of the parameters λ_1, λ_2, $\lambda_{\max}$, λ_{01}, λ_{02}, and λ_{03} used in Eqs. (9–11), we considered eight cases. In each case, the parameters λ_{0j} ($j = 1, 2, 3$) were defined as follows:

$$\lambda_{01} = \beta_1\lambda_1, \qquad \lambda_{02} = \lambda_1 + \beta_2(\lambda_2 - \lambda_1)$$
$$\lambda_{03} = \lambda_2 + \beta_3(\lambda_{\max} - \lambda_2) \tag{17}$$

The parameters are presented in Table 1. Note that the first and third domains in the table are relatively small. The motivation was to have more collocation points at the ends of the reaction zone to resolve possible oscillations in the eigenfunctions and to resolve accurately region $\lambda \to 1$. In all cases, we used an equal number of collocation points: $N_1 = N_2 = N_3 = N$. Figure 1 shows results obtained in case 1 with $N = 50$, $N = 100$, and $N = 200$ at the reaction and flow parameters $\gamma = 1.2$, $E = 100$, $Q = 50$, and $f = 1.2$. This is an example of the high activation energy considered in [5].

Table 1 Parameters used in the test cases

	λ_1	λ_2	$\lambda_{\max}$	β_1	β_2	β_3
Case 1	0.1	0.9	0.9995	0.55	0.55	0.9
Case 2	0.1	0.8	0.9995	0.55	0.55	0.9
Case 3	0.1	0.9	0.9995	0.55	0.55	0.7
Case 4	0.1	0.9	0.9995	0.55	0.55	0.99
Case 5	0.2	0.9	0.9995	0.55	0.55	0.9
Case 6	0.1	0.9	0.99995	0.55	0.55	0.9
Case 7	0.1	0.9	0.995	0.55	0.55	0.9
Case 8	0.05	0.9	0.9995	0.55	0.55	0.9

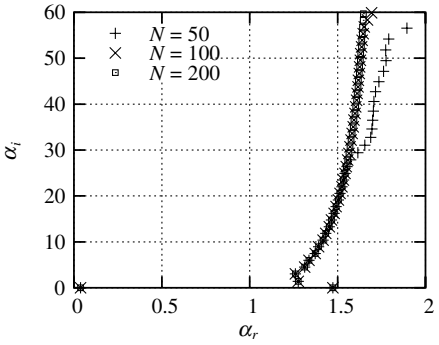

Fig. 1 Comparison of eigenvalue maps at $N = 50$, $N = 100$, and $N = 200$ for case 1; $f = 1.2$, $Q = 50$, $E = 100$.

The computations required about 25, 230, and 2100 s on a Dell Optiplex GX620 at $N = 50$, $N = 100$, and 200, respectively.

Because eigenvalues at $Re(\alpha) < 0$ are not physical (they represent spatially unbounded solutions), only results with $Re(\alpha) > 0$ are presented. We have to mention that the algorithm generates a spurious eigenvalue $\alpha = 0$ that corresponds to the solution of Eq. (5) with $\psi \neq 0$ and $z = 0$ (this eigenvalue is removed from the plots).

Figures 2 and 3 demonstrate comparisons of cases 1–8 at $N = 100$. One may conclude from Fig. 2 that an increase of the first interval in case 5 ($\lambda_1 = 0.2$) leads to poor convergence at large $\mathrm{Im}(\alpha)$. This is attributed to an insufficient number of collocation points on the interval. Decrease of the first interval in case 8 ($\lambda_1 = 0.05$) also leads to divergence at $\mathrm{Im}(\alpha)$ about 50 (Fig. 3). This is attributed to an insufficient number of collocation points on the second interval.

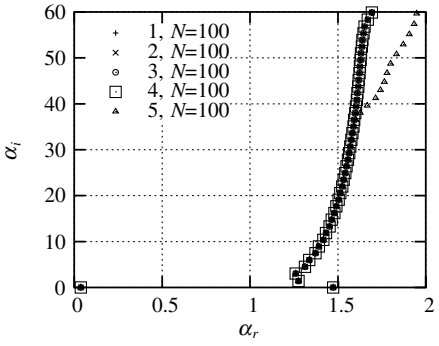

Fig. 2 Comparison of eigenvalue maps at $\gamma = 1.2$, $f = 1.2$, $Q = 50$, and $E = 100$; cases 1–5.

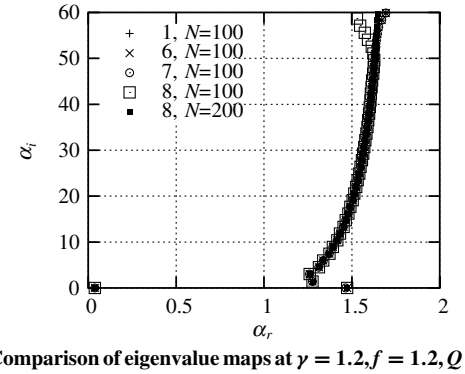

Fig. 3 Comparison of eigenvalue maps at $\gamma = 1.2$, $f = 1.2$, $Q = 50$, and $E = 100$; cases 1, 6, 7, and 8.

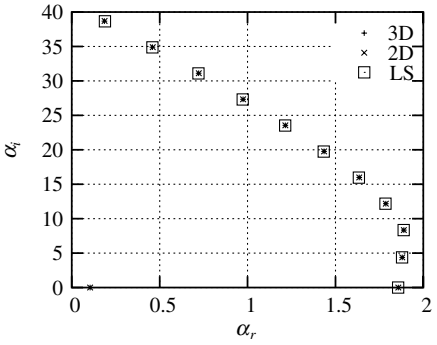

Fig. 4 Comparison of eigenvalue maps for $f = 1$, $\gamma = 1.2$, $Q = 50$, $E = 50$: 2D = two-domain method; 3D = three-domain method; LS=[4]. The eigenvalues are scaled with the half-reaction time $t_{1/2}$.

Table 2 Comparison of the unstable discrete spectrum of Lee and Stewart [4] and present work (eigenvalues are scaled with $t_{1/2}$)

		[4]		present work	
f	Mode no.	α_r	α_i	α_r	α_i
1	1	1.857	0.000	1.85837	0.000000
	2	1.879	4.372	1.88055	4.37622
	3	1.888	8.333	1.88974	8.34094
	4	1.785	12.16	1.78689	12.1663
	5	1.634	15.96	1.63560	15.9714
	6	1.434	19.74	1.43583	19.7614
	7	1.214	23.53	1.21542	23.5476
	8	0.973	27.31	0.974337	27.3327
	9	0.721	31.09	0.721998	31.1176
	10	0.459	34.87	0.459270	34.9005
	11	0.189	38.65	0.185795	38.6889
1.2	1	0.569	0.300	0.568874	0.299575
	2	1.148	4.547	1.14774	4.54785
	3	0.933	8.234	0.933278	8.23523
	4	0.550	11.84	0.549969	11.8456
	5	0.095	15.44	0.0951347	15.4406
1.4	1	0.313	0.664	0.313410	0.664483
	2	0.504	4.484	0.504564	4.48421
1.6	1	0.112	0.789	0.111763	0.788817
1.731	1	0.000	0.825	-1.01658×10^{-4}	0.825109

Figure 3 also shows results for case 8 at $N = 200$, which are the same as for case 1 with $N = 200$ shown in Fig. 1.

Finally, we compare results obtained with the help of the two- and three-domain spectral collocation methods. In the two-domain computations, the second domain was the same as the third domain in the three-domain case. The first domain was stretched from $\lambda = 0$ to 0.9 with λ_{01} in Eq. (9) equal to 0.55×0.9. In both methods, $N = 100$ was used for each domain. Figure 4 demonstrates comparisons of the two- and three-domain results, together with eigenvalues published in [4] at $f = 1$, $E = Q = 50$, and $\gamma = 1.2$. In Fig. 4, the eigenvalues are scaled with the half-reaction time $t_{1/2}$,

$$\frac{t_{1/2}}{t_c} = \frac{\int_0^1 (1-\lambda^*)^{-1} \exp(\theta/p^*v^*)\, \mathrm{d}\lambda^*}{\int_0^1 u^*(1-\lambda^*)^{-1} \exp(\theta/p^*v^*)\, \mathrm{d}\lambda^*} \tag{18}$$

One can see that for these particular parameters the agreement is very good. The two-domain method required only about 70 s of computational time, in contrast to the three-domain method, where 230 s were required. It means that the two-domain version of the spectral collocation method should be preferable when moderate frequencies $\mathrm{Im}(\alpha)$ of the perturbations are of interest. Although the numerical implementation deals with the constraint, Eq. (7), imposed at $\lambda = \lambda_{\max} < 1$ and matrix $\mathbf{A}^*$ is still nonsingular at $\lambda = \lambda_{\max}$, we should interpret the result as a limit at $f \to 1$ because the derivation of the constraint was based on consideration of overdriven detonations.

Table 2 is a comparison of the results from [4] and the present work (three-domain spectral collocation method, $N = 100$). This table also shows that the results found in the present work are almost the same as the results obtained from Erpenbeck's dispersion relation in [9] using the solution of the adjoint system together with a shooting algorithm.

It is worthwhile to note that the generalized eigenvalue problem has exposed the eigenvalue $\alpha = 0.10191$ in Fig. 4, whereas the eigenvalue was lost in the carpet search used in [4] (not included in Table 2). The missed eigenvalue was found by Short [5].

One can find other examples with the application of the multidomain spectral collocation method in [9].

IV. Conclusions

The numerical results obtained with the help of the multidomain spectral collocation method for the stability of detonations demonstrate that the method is very robust, and that it should replace the archaic carpet search. For practical applications dealing with many reactions, one can easily reformulate the method in terms of the spatial coordinate x instead of the reaction progress variable λ.

Acknowledgment

The author thanks the anonymous reviewer for helpful comments and suggestions.

References

[1] Erpenbeck, J. J., "Stability of Steady-State Equilibrium Detonations," *Physics of Fluids*, Vol. 5, No. 5, 1962, pp. 604–614.

[2] Erpenbeck, J. J., "Stability of Idealized One-Reaction Detonations," *Physics of Fluids*, Vol. 7, No. 5, 1964, pp. 684–696.

[3] Fickett, W., and Davis, W. C., *Detonation: Theory and Experiment*, Dover, New York, 2000; republication of the original work published in 1979 by the Univ. of California Press, Berkley, CA.

[4] Lee, H. I., and Stewart, D. S., "Calculation of Linear Detonation Instability: One-Dimensional Instability of Plane Detonation," *Journal of Fluid Mechanics*, Vol. 216, No. 1, 1990, pp. 103–132.

[5] Short, M., "Multidimensional Linear Stability of a Detonation Wave at High Activation Energy," *SIAM Journal on Applied Mathematics*, Vol. 57, No. 52, 1997, pp. 307–326.

[6] Short, M., and Stewart, D. S., "Cellular Detonation Stability, Part 1: a Normal-Mode Linear Analysis," *Journal of Fluid Mechanics*, Vol. 368, 1998, pp. 229–262.

[7] Kasimov, A. R., and Stewart, D. S., "Spinning Instability of Gaseous Detonations," *Journal of Fluid Mechanics*, Vol. 466, 2002, pp. 179–203.

[8] Kasimov, A. R., *Theory of Instability and Nonlinear Evolution of Self-Sustained Detonation Waves*, Ph.D. Thesis, Univ. of Illinois at Urbana–Champaign, Urbana, IL, 2004.

[9] Tumin, A., "Stability of Idealized One-Reaction Detonations Revisited," AIAA Paper 2007-0987, 2007.

[10] Buckmaster, J., and Neves, J., "One-Dimensional Detonation Stability: the Spectrum for Infinite Activation," *Physics of Fluids*, Vol. 31, No. 12, 1988, pp. 3571–3576.

[11] Namah, G. S., Brauner, C., Buckmaster, J., and Schmidt-Laine, C., "Linear Stability of One-Dimensional Detonations," *Dynamical Issues in Combustion Theory*, edited by A. Friedman and W. Miller Jr., IMA Volumes in Mathematics and its Applications, Vol. 35, Springer–Verlag, New York, 1991, pp. 229–239.

[12] Malik, M. R., "Numerical Methods for Hypersonic Boundary Layer Stability," *Journal of Computational Physics*, Vol. 86, No. 2, 1990, pp. 376–413.

[13] Canuto, C., Hussaini, M. Y., Quarteroni, A., and Zang, T. A., *Spectral Methods in Fluid Dynamics*, Springer–Verlag, Berlin, 1988.

[14] Hanifi, A., Schmid, P. J., and Henningson, D. S., "Transient Growth in Compressible Boundary Layer Flow," *Physics of Fluids*, Vol. 8, No. 3, 1996, pp. 826–837.

C. Kaplan
Associate Editor